Capability of Nano-hydroxyapatite Gel on Remineralization of Enamel and Cementum Around Margin of Computer-Aided Design and Computer-Aided Manufacturing Ceramic Restoration

ผลของนาโนไฮดรอกซีอะพาไทต์เจลในการคืนแร่ธาตุสู่เคลือบฟันและเคลือบรากฟันบริเวณพื้นผิวของขอบวัสดุชนิดเซรามิกประเภทแคด/แคม

Preeyarat Plongniras (ปรียารัตน์ ปล่องนิราส)* Dr.Niwut Juntavee (ดร.นิวัตร จันทร์เทวี)**
Dr.Apa Juntavee (ดร.อาภา จันทร์เทวี)*** Dr.Supaporn Chatrchaiwiwatana (ดร.สุภาภรณ์ ฉัตรชัยวิวัฒนา)****

ABSTRACT

This study investigated into the effects of nanohydroxyapatite (NHA) gel and Clinpro (CP) on the remineralization of enamel and cementum at their cavosurface areas of CAD-CAM ceramic restorations. Thirty extracted mandibular third molars were sectioned at 1-mm above and below the cemento-enamel junction (CEJ). By a bonding process with a resin cement (25-micron cement film thickness), their crown-CEJ-root portions were replaced with an ytria-stabilized zirconia polycrystalline. A 4x4 mm^2 area surrounding the ceramic disk was demineralized and further treated with either NHA or CP, while one group was left untreated in deionized water. Enamel's and cementum's microhardness values were determined before demineralization, after demineralization, and after remineralization. The result indicated some significant increases of the microhardness of the demineralized enamel and cementum upon an application of either NHA or CP (p <0.05). Those with NHA indicated a higher remineralization capability than those with CP (p<0.05). NHA and CP were capable of some remineralizations on enamel and cementum around the finishing line of CAD-CAM ceramic. NHA was extremely potential in the remineralization processes and was recommended for an early therapeutic fixed reconstruction.

บทคัดย่อ

การศึกษานี้ได้ทดสอบผลของนาโนไฮดรอกซีอะพาไทต์เจลและคลินโปร ในการคืนแร่ธาตุสู่เคลือบฟันและเคลือบรากฟันบริเวณพื้นผิวของขอบวัสดุชนิดเซรามิกประเภทแคด/แคม ฟันกรามซี่ที่สามในขากรรไกรล่างซึ่งถูกถอนจำนวน 30 ซี่ ได้ถูกตัด ณ ตำแหน่ง 1 มม. เหนือต่อและใต้ต่อรอยต่อเคลือบฟันกับเคลือบรากฟัน แล้วส่วนดังกล่าวถูกแทนที่ด้วยชิ้นเซอร์โคเนีย โดยยึดกับฟันด้วยเรซินซีเมนต์ (หนา 25 ไมครอน) เตรียมระนาบขนาด 4x4 มม^2 รอบชิ้นเซรามิกซึ่งทำให้เกิดรอยผุเทียม แล้วทาด้วยนาโนไฮดรอกซีอะพาไทต์หรือคลินโปร ในขณะที่อีกกลุ่มหนึ่งถูกแช่ในน้ำซึ่งปราศจากไอออนโดยไม่ได้รับสารใด ทดสอบความแข็งผิวระดับจุลภาคของเคลือบฟันและเคลือบรากฟันก่อนและหลังทำให้เกิดรอยผุเทียม และวัดหลังการทาสาร

* Student, Master of Science Program in Prosthodontics, Faculty of Dentistry, Khon Kaen University
** Associate Professor, Department of Prosthodontics, Faculty of Dentistry, Khon Kaen University
*** Associate Professor, Department of Pediatric dentistry, Faculty of Dentistry, Khon Kaen University
**** Associate Professor, Department of Community dentistry, Faculty of Dentistry, Khon Kaen University

ผลการศึกษาพบว่า นาโนไฮดรอกซีอะพาไทต์และคลินโปรสามารถคืนแร่ธาตุแก่เคลือบฟันและเคลือบรากฟันที่มีรอยผุเทียมอย่างมีนัยสำคัญทางสถิติ ที่ระดับนัยสำคัญ 0.05 โดยนาโนไฮดรอกซีอะพาไทต์สามารถคืนแร่ธาตุสูงกว่าคลินโปรอย่างมีนัยสำคัญทางสถิติ ที่ระดับนัยสำคัญ 0.05

จึงสรุปได้ว่านาโนไฮดรอกซีอะพาไทต์และคลินโปรสามารถส่งเสริมการคืนแร่ธาตุบริเวณผิวเคลือบฟันและเคลือบรากฟัน บริเวณพื้นผิวของขอบวัสดุชนิดเซรามิกประเภทแคด/แคม นาโนไฮดรอกซีอะพาไทต์มีความสามารถสูงมากในกระบวนการคืนแร่ธาตุและได้ถูกแนะนำสำหรับการรักษาเบื้องต้นในการบูรณะชนิดติดแน่น

Keywords: Nanohydroxyapatite, Remineralization, CAD-CAM

คำสำคัญ: นาโนไฮดรอกซีอะพาไทต์ การคืนแร่ธาตุ แคด-แคม

Introduction

Esthetic dentistry is considerably increasing, which is leading the ceramic to be a material of preferred choices in restorative dentistry domain. The technological advancements in the computer-aided designed (CAD) and computer aided manufacturing (CAM) in dentistry has been commenced by clinicians and researchers for developing new ceramic materials, which can render high quality and reliable restorations along with good prognosis. Several types of ceramic materials have been developed to meet the both the patients' and dentists' demands for highly esthetics and natural appealing restorations. Several ceramic-based materials have been recently introduced for the CAD-CAM technology including resin nano ceramic, hybrid ceramic, lithium disilicate glass ceramic, ytria-stabilized tetragonal zirconia polycrystalline (Y-TZP), monolithic zirconia, and zirconia-reinforce lithium silicate ceramic (Denry and Kelly, 2014). These newly developed ceramic restorative materials are the fruit of the revolution in the technological approaches. These approaches offer the appropriate ceramic material properties to clinicians for different treatment procedures, for providing the ease of restoration fabrication via CAD-CAM technology. However, the ceramic restorative material's accuracy is still compromised in comparison to metal ceramic restoration (Felton et al., 1991; Han et al., 2017). Improper marginal adaptation of dental restoration induces micro-bacteria deposition on the plaque, which initiates periodontal disease and decay leading to the failure of restoration (Felton et al., 1991; Han et al., 2017). Underprivileged marginal fit of CAD-CAM restoration often causes decay around the finishing line of restoration, which is generally placed on the enamel, close to the cement-enamel junction (CEJ). However, the finishing line is occasionally placed on the cementum, close to the CEJ in the advanced reconstruction of the periodontal involvement dentition using fixed prosthesis. Long-term clinical success of ceramic restoration was influenced by restorative margin's accuracy to be adapted to the finishing line, which is placed on either cementum or enamel.

Dental caries is a dietary carbohydrate-modified bacterial infectious disease, and is one of the most common bacterial infection in humans. It is a threat to oral and systemic health, and creates a heavy financial burden worldwide (Hu et al., 2011). The basic mechanism of dental caries is demineralizing through the attack by acids generated by bacteria in dental plaque biofilms (Featherstone, 2004). Approximately, 200 million teeth having restorations placed annually with increasingly used ceramic for reconstruction (Cheng et al., 2015). The ceramic restorations are bonded to the teeth using resin adhesive, which tend to accumulate biofilms more than other restorative procedures (Cheng et al., 2013). Dental plaque adjacent to the restoration margins may facilitate the development of secondary caries and compromise the restoration longevity. Indeed, secondary caries around the restorative margins has been considered to be a primary reason for failure of the fixed prosthodontics, thus, limiting the longevity of restorations(Mjor, 2005; Ten Cate, 2012). It was reported that 18–22% of the fixed prostheses' abutments was affected by dental caries, leading to the endodontic treatment and new prostheses replacement (Walton et al., 1986; Goodacre et al., 2003; Raigrodski, 2004). Dental caries underneath a restorative margin either on enamel or on cementum portion is hardly detectable by radiograph. Delayed detection of dental caries underneath a restorative margin leads to irreversible pulp involvement (Gordan et al., 2009). Caries around the margin of fixed prosthesis are relatively associated with the leakage through the margin of restoration, which progresses with the luting cement's dissolution (Mjor, 2005; Zoellner et al., 2002). It is related with the incidence of root caries in the elderly people, and teeth with sclerotic dentin (González-Cabezas, 2010; Ioannidis et al., 2010; Klarić et al., 2013; Petersson, 2013; Schüpbach et al., 1992).

The prevention of secondary caries occurrence around the restorative margin was signified by the concept of remineralization and demineralization of tooth surface (Hoceini et al., 2016). Remineralizing agents proceed in various forms, such as restorative materials, fissure sealants, chewing gums, mouth rinses and dentifrices (Li et al., 2014; Malekafzali et al., 2015; Weir et al., 2012). One of the most effective remineralizing agents in caries prevention is fluoride. Nevertheless, some concerns have been expressed about fluorosis and excess fluoride intake (Li et al., 2014; Malekafzali et al., 2015). In the recent years, fluoride's alterative materials have been introduced, including CPP-ACP and nano-hydroxyapatite (NHA), because of their anticariogenic properties (Kalra et al., 2014; Vyavhare et al., 2015). NHA that contains calcium and phosphate crystal has similar characteristics to human's hard tissue, has received huge attention in the medical and dentistry domain because of nanotechnology. This nanotechnology has been reported to provide novel prevention strategies and treatment of dental caries, specifically in the control and management of dental plaque biofilm and remineralization of initial dental caries (Hannig and Hannig, 2010). Nanoparticles are generally considered a size reduced from microns to nanometers, which can dramatically change the resultant properties, such as hardness, active surface area, chemical reactivity and biological activity (Allaker and Ren, 2008). Nanoparticles were applied in restorative dentistry in the form of remineralizing agents (Hannig and Hannig, 2012). Several remineralization materials are available that are based on nanotechnological approaches have been reported for the remineralization process of early carious lesions (Naik et al., 2017; Oliveby et al., 1990). NHA is also considered one of the most biocompatible and bioactive materials used in medicine and dentistry in recent years(Hannig and Hannig, 2010; Lv et al., 2007). NHA at a concentration of 10% is capable of remineralization process on enamel surface (Huang et al., 2009; Pepla et al., 2014; Vyavhare et al., 2015). Some studies have reported more or comparable remineralizing effects for NHA toothpaste to other toothpaste containing amino-fluoride and fluoride (Tschoppe et al., 2011). It was reported that NHA of particle size 10–20 nm in diameters, and 60–80 nm in length can promote penetration of crystal into the interprismatic space through ion transportation and presumably affiliated to the interprismatic protein, resulting in remineralization on the superficial layer of artificial carious lesions, and possibly reverse the progression of initial caries lesions (Baumann et al., 2015; Huang et al., 2010; Kunin et al., 2015; Lubarsky et al., 2014; Moradian-Oldak, 2012; Ruan and Moradian-Oldak, 2015; Wang et al., 2017). However, there are no reported cases till date regarding the present study's use of any NHA in gel preparation on the early therapeutic aspect in restorative dentistry. This study was aimed to investigate the effects of NHA gel and CP on remineralization potential of enamel and cementum at the cavosurface area of CAD-CAM ceramic restoration.

Material and Methods

The *in vitro* study was conducted with the ethically approved on exemption from the Ethics Committee in Human Research (Reference No: HE 592239) at Khon Kaen University. Thirty extracted human mandibular third molars were selected for this study. The samples were sectioned with precision machine (Isomet 4000®, Buehler, IL, USA) at 1 mm above and below the cemento-enamel junction (CEJ), dividing it into crown (C), crown-CEJ-root (CCR), and root (R) portions (Figure 1A, (1)). The CCR portion was removed and replaced with ceramic disk with the same dimension and shape. The CCR portion was used as a prototype for fabrication of a ceramic disk (2 mm in thickness) (Figure 1A, (2)). The partial-sintered Y-TZP blank (in Coris® TZI, Dentsply Sirona, York, PA, USA) was prepared in a disk shape with similar contour as CCR portion, but was 20% wider in size to compensate for sintering shrinkage of zirconia. The ceramic disk was further sintered in the furnace (inFire® HTC speed, Densply Sirona, Charlotte, NC, USA), according to the manufacturer's instructions at 1510°C for 2 hours, to derive precise ceramic thickness of 1.6 mm with exactly similar contour with the CCR portion. The ceramic disk was bonded in between the C and R portion of each tooth using resin cement (Super-Bond C&B, Sun Medical, Shiga, Japan) with controlled cement film thickness that needed to be 25 microns, using digital veneer caliper (Mitutoyo, Boulevard Aurora, IL, USA) (Figure 1A, (3)). The cement was auto-polymerized and it took the cement 10 minutes to reach full polymerization state. The sample was invested in the acrylic block (Unifast Trad, GC corp., Tokyo, Japan) and left exposed at the surface for further experimentation (Figure 1A, (4)). A flat surface of 4x4 mm^2 was created on the sample's exposed surface, using Ecomet 3® Machine (Buehler, IL, USA) (Figure 1A, (5)). The samples were washed, and stored in deionized water at 37°C for 24 hours.

Demineralized gel for artificial carious formation was prepared in synthetic polymer gel, which comprised of 20 grams/liter of carbopol 907 (BF Goodrich Co., Cleveland, OH, USA), and mixed with 0.2% polyacrylic acid and 0.1% lactic acid, and adjusted pH to 4.4 by sodium hydroxide. The samples were immersed in a demineralized gel, stored in the humidified environment for 16 hours, and rinsed with deionized water.

The samples were randomly divided into three groups (n=10), to be treated with either nanohydroxyapatite (NHA) gel or Clinpro (CP) tooth crème, while one group was left in deionized water (no treatment) and served as a control (NT). Each remineralized agent was applied onto the demineralized surface of enamel and cementum, covering the area 4x4 mm^2, and was left for 4 minutes prior to immersion in freshly prepared deionized water. The remineralized gels were applied twice a day, with 12 hours interval, for a period of 30 days.

The surface microhardness of the tooth was determined for microhardness by indenting with Vickers indenter at 100 grams load for enamel and 10 grams load for cementum for 15 seconds as the dwelling time using microhardness tester (Future-tech, FM-800, Tokyo, Japan). The microhardness on enamel and cementum was determined at the distance of 40 microns above and below the resin-enamel, respectively. The microhardness was determined before the application of demineralized solution (B_D), which served as the baseline data, after the application of demineralized solution (A_D) and remineralized gel (A_R). Each indentation was randomly determined at 100 µ from each other (Figure 2).

Sample from each group was evaluated and compared for surface alteration of area surrounding the ceramic disk at different stages, which included before demineralized (B_D), after demineralized (A_D) and after remineralized (A_R) stages. The sample was later coated with gold in sputter coater machine (Emitech, K500X, East Grinstead, England), and evaluated in the scanning electron microscope (SEM, S-3000N, Hitachi, Tokyo, Japan).

Results

The results of the remineralization on both the enamel and cementum area surrounding the margin of CAD-CAM ceramic restoration based on surface microhardness are reported in Figure 3 and Table 1. The surface microhardness values (mean ± standard deviation) for control group (NT) at B_D, A_D, and A_R were 377.37 ± 22.99, 161.95 ± 10.54, and 161.70 ± 5.92 for enamel, and 60.37 ± 3.81, 17.65 ± 0.91, and 17.04 ± 1.00 for cementum, respectively. The surface microhardness values (mean ± standard deviation) for nano-hydroxyapatite group (NHA) at B_D, A_D, and A_R were 378.20 ± 18.76, 160.72 ± 8.38, and 200.08 ± 8.29 for enamel, and 62.58 ± 3.37, 18.38 ± 1.33, and 27.99 ± 2.68 for cementum, respectively. The surface microhardness values (mean ± standard deviation) for Clinpro group (CP) B_D, A_D, and A_R were 380.53 ± 25.14, 161.94 ± 5.66, and 193.16 ± 7.54 for enamel, and were 62.78 ± 4.75, 19.07 ± 1.30, and 24.46 ± 2.02 for cementum, respectively.

An analysis of variance indicated a significant difference in surface hardness for both the enamel and cementum area surrounding the ceramic because of different remineralizing materials and stages of material application ($p<0.05$), but no significant difference in surface hardness upon the interaction of the material and stage of the application was found ($p>0.05$), as shown in Table 2. The *post hoc* multiple comparison indicated significant difference in the capability of remineralization effect to the demineralized surface of either enamel or cementum area surrounding the CAD-CAM ceramic restoration for both the NHA and CP in comparisons to no treatment group (NT) ($p<0.05$), as shown in Table 3. There was significant difference in the remineralization capability between NHA and CP to the demineralized surface of the enamel and cementum area surrounding the ceramic restoration ($p<0.05$) as shown in Table 3. The NHA indicated higher capability in remineralization to the demineralized surface of either enamel or cementum area surrounding the ceramic than the CP ($p<0.05$), as shown in Table 3 and Figures 3A and 3B.

The SEM photomicrographs indicated generalized smooth surface architecture of both the enamel (Figure 4A) and cementum, when compared to those without treatment (Figure 4B). Generalized surface irregularities characteristics were denoted on the surface of demineralized enamel (Figure 4C). Generalized irregularities of cementum with opening tubules were found after the demineralized process (Figure 4D). The surface architecture of enamel exhibited smoother area after the NHA (Figure 4G) and CP (Figure 4I) were applied for 30 days, when compared to those without treatment in enamel (Figure 4E) and cementum (Figure 4F). The micrographs revealed that the NHA particles deposition in the tubules of cementum, as well as generalized reduction of surface irregularities, were denoted (Figure 4H). On the other hand, some CP particles were found to be partially deposited in the cementum's tubules with minimal irregularities of the surfaces (Figure 4J).

Discussion

Absolutely integrated tooth-restoration junction is an important goal that is hardly achieved. Indeed, irregularities at cavosurface junction and micro-gaps at the tooth-restoration interfaces are always present and induce bacterial accumulation leading to tooth decay. Therefore, remineralization concept on the restoration-tooth junction is a preventive mean in restorative dentistry in the next decade. The study indicated that both NHA and CP were significantly capable of remineralization to recover the demineralized enamel and cementum in comparison to the non-treated demineralized surface ($p<0.05$). The NHA indicated significantly higher capability in remineralization the demineralized surface of both the enamel and cementum than CP ($p<0.05$). This possibly indicated ion transportation in the remineralization process (Kunin et al., 2015). This also related with isomorphic and isoionic exchange process in enamel crystals that occurred upon the diffusion of calcium and phosphate through the interprismatic spaces and turned into hydroxyapatite crystals (Kunin et al., 2015). The NHA significantly has a higher capability in remineralization than CP, and this is possibly related to the NHA's nano-particle, which is susceptible with tooth structure. NHA is able to enhance penetration of its crystals through the interprismatic spaces of enamel and results in the formation of the hydroxyapatite crystals (Kunin et al., 2015). The calcium, phosphate and fluoride composition in CP could only replace the lost mineral, by forming fluoroapatite crystal in the remineralization process (Oliveby et al., 1990).

The demineralized enamel surface was considerably rough and slightly porous (Klarić et al., 2013). This facilitated the NHA to penetrate into the interprismatic spaces because of the precipitation process. It also attracted a large amount of Ca^{2+} and PO_4^{3-} from the saturated solution at the outer layer of enamel surface to re-fill the vacant positions of the crystals (Huang et al., 2009; Lv et al., 2007). The demineralization of cementum clearly showed the surface's exposed tubules. The mineral depositions were found in the tubules as a contributing remineralization effect (González-Cabezas, 2010; Schüpbach et al., 1992). The remineralization of cementum upon using NHA and CP is possibly associated with the exchange of minerals between cementum and surrounding environment as is found in the enamel. However, the remineralization process in cementum is less effective than in enamel. The higher capability in remineralization in cementum for NHA as compared to CP is possibly associated with the nano-particle size that is capable of constructive interdigitation upon the cementum structure (Moradian-Oldak, 2012; Ruan and Moradian-Oldak, 2015).

The deionized water was used as alternative to artificial saliva to eliminate the confounding factors that could be from other contents, such as amino acids components in salivary protein that possibly effect to natural enamel matrix proteins of tooth specimens (Vyavhare et al., 2015). In addition, minerals in artificial saliva may affect the confounding factors during remineralized process, as the deproteination of enamel results in a significant reduction of enamel resistant and characteristics (Baumann et al., 2015). However, this study indicated that NHA provides strong evidence on surface remineralization capability for the enamel and cementum surrounding the ceramic restoration.

Conclusion

The application of NHA to combat dental caries through the demineralization and remineralization balance is relatively new paradigm of preventive approach in restorative dentistry. In the view of recurrent caries at the tooth-restoration margin as the main factor for restoration failure, the NHA and CP showed effective capabilities of remineralization for the enamel and cementum surrounding the finishing area of CAD-CAM restoration, which resulted in effective caries inhibition. NHA was capable of exhibiting remineralization better than CP for using in the remineralization process of both in the enamel and cementum. The novel NHA gel indicated promising early therapeutics aspect in restorative dentistry, and was addressed as philosophy in caries prevention in fixed prosthodontics reconstruction. Further clinical study is needed to determine the efficacy of using NHA gel in daily clinical practice.

References

Allaker RP , Ren G. Potential impact of nanotechnology on the control of infectious diseases. Trans R Soc Trop Med Hyg 2008; 102(1): 1-2.

Baumann T, Carvalho T, Lussi A. The effect of enamel proteins on erosion. Sci Rep 2015; 5: 15194.

Cheng L, Weir MD, Zhang K, Arola DD, Zhou X , Xu HH. Dental primer and adhesive containing a new antibacterial quaternary ammonium monomer dimethylaminododecyl methacrylate. J Dent 2013; 41(4): 345-355.

Cheng L, Zhang K, Weir MD, Melo MAS, Zhou X, Xu HH. Nanotechnology strategies for antibacterial and remineralizing composites and adhesives to tackle dental caries. Nanomedicine (Lond) 2015; 10(4): 627-641.

Denry I, Kelly J. Emerging ceramic-based materials for dentistry. J Dent Res 2014; 93(12): 1235-1242.

Featherstone J. The continuum of dental caries—evidence for a dynamic disease process. J Dent Res 2004; 83 (Spec No C:C): 39-42.

Felton D, Kanoy B, Bayne Sa, Wirthman G. Effect of *in vivo* crown margin discrepancies on periodontal health. J Prosthet Dent 1991; 65(3): 357-364.

González-Cabezas C. The chemistry of caries: remineralization and demineralization events with direct clinical relevance. Dent Clin North Am 2010; 54(3): 469-478.

Goodacre CJ, Bernal G, Rungcharassaeng K, Kan JY. Clinical complications in fixed prosthodontics. J Prosthet Dent 2003; 90(1): 31-41.

Gordan VV, Garvan CW, Heft MW, Fellows JL, Qvist V, Rindal DB, Gilbert GH , Group DC. Restorative treatment thresholds for interproximal primary caries based on radiographic images: findings from the dental practice-based research network. Gen Dent 2009; 57(6): 654.

Han J, Zhao J, Shen Z. Zirconia ceramics in metal-free implant dentistry. Adv Appl Cer 2017; 116(3): 138-150.

Hannig M , Hannig C. Nanomaterials in preventive dentistry. Nat Nanotechnol 2010; 5(8): 565-569.

Hannig M , Hannig C. Nanotechnology and its role in caries therapy. Adv Dent Res 2012; 24(2): 53-57.

Hoceini A, Khelil NK, Ben-Yelles I, Mesli A, Ziouani S, Ghellai L, Aissaoui N, Nas F , Arab M. Caries-related factors and bacterial composition of supragingival plaques in caries free and caries active Algerian adults. Asian Pac J Trop Med 2016; 6(8): 720-726.

Hu D-y, Hong X, Li X. Oral health in China–trends and challenges. Int J Oral Sci 2011; 3(1): 7-12.

Huang S, Gao S, Cheng L, Yu H. Combined effects of nano-hydroxyapatite and *Galla chinensis* on remineralisation of initial enamel lesion *in vitro*. J Dent 2010; 38(10): 811-819.

Huang S, Gao S, Yu H. Effect of nano-hydroxyapatite concentration on remineralization of initial enamel lesion *in vitro*. Biomed Mat 2009; 4(3): 034104.

Ioannidis G, Paschalidis T, Petridis H, Anastassiadou V. The influence of age on tooth supported fixed prosthetic restoration longevity. A systematic review. J Dent 2010; 38(3): 173-181.

Kalra DD, Kalra RD, Kini PV, Prabhu CA. Nonfluoride remineralization: An evidence-based review of contemporary technologies. J Dent Allied Sci 2014; 3(1): 24-33.

Klarić E, Marcius M, Ristić M, Sever I, Prskalo K, Tarle Z. Surface changes of enamel and dentin after two different bleaching procedures. Acta clin Croat 2013; 52(4): 413-428.

Kunin AA, Evdokimova AY, Moiseeva NS. Age-related differences of tooth enamel morphochemistry in health and dental caries. EPMA J 2015; 6(1): 3.

Li X, Wang J, Joiner A, Chang J. The remineralisation of enamel: a review of the literature. J Dent 2014; 42: S12-20.

Lubarsky GV, Lemoine P, Meenan BJ, Deb S, Mutreja I, Carolan P, Petkov N. Enamel proteins mitigate mechanical and structural degradations in mature human enamel during acid attack. Mater Res Express 2014; 1(2): 025404.

Lv KL, Zhang JX, Meng XC, Li XY. Remineralization effect of the nano-HA toothpaste on artificial caries. Key Eng Mater 2007. Trans Tech Publ, 267-270.

Malekafzali B, Ekrami M, Mirfasihi A , Abdolazimi Z. Remineralizing Effect of child formula dentifrices on artificial enamel caries using a pH cycling model. J Dent (Tehran) 2015; 12(1): 11-17.

Mjor IA. Clinical diagnosis of recurrent caries. J Am Dent Assoc 2005; 136(10): 1426-1433.

Moradian-Oldak J. Protein-mediated enamel mineralization. Front Biosci (Landmark Ed) 2012; 17: 1996-2023.

Naik NS, Reddy VS, Shashikiran N. Comparative evaluation of secondary caries formation around light-cured fluoride-releasing restorative materials. J Indian Soc Pedod Prev Dent 2017; 35(1): 75-82.

Oliveby A, Twetman S, Ekstrand J. Diurnal fluoride concentration in whole saliva in children living in a high-and a low-fluoride area. Caries Res 1990; 24(1): 44-47.

Pepla E, Besharat LK, Palaia G, Tenore G, Migliau G. Nano-hydroxyapatite and its applications in preventive, restorative and regenerative dentistry: a review of literature. Ann Stomatol 2014; 5(3): 108-114.

Petersson LG. The role of fluoride in the preventive management of dentin hypersensitivity and root caries. Clin Oral Investig 2013; 17(1): 63-71.

Raigrodski AJ. Contemporary materials and technologies for all-ceramic fixed partial dentures: a review of the literature. J Prosthet Dent 2004; 92(6): 557-562.

Ruan Q, Moradian-Oldak J. Amelogenin and enamel biomimetics. J Mater Chem B Mater Biol Med 2015; 3(16): 3112-3129.

Schüpbach P, Lutz F, Guggenheim B. Human root caries: histopathology of arrested lesions. Caries Res 1992; 26(3): 153-164.

Ten Cate J. Novel anticaries and remineralizing agents: prospects for the future. J Dent Res 2012; 91(9): 813-815.

Tschoppe P, Zandim DL, Martus P, Kielbassa AM. Enamel and dentine remineralization by nano-hydroxyapatite toothpastes. J Dent 2011; 39(6): 430-437.

Vyavhare S, Sharma DS, Kulkarni V. Effect of three different pastes on remineralization of initial enamel lesion: an *in vitro* study. J Clin Pediatr Dent 2015; 39(2): 149-160.

Walton JN, Gardner FM, Agar JR. A survey of crown and fixed partial denture failures: length of service and reasons for replacement. J Prosthet Dent 1986; 56(4): 416-421.

Wang H, Xiao Z, Yang J, Lu D, Kishen A, Li Y, Chen Z, Que K, Zhang Q, Deng X, Yang X, Cai Q, Chen N, Cong C, Guan B, Li T , Zhang X. Oriented and ordered biomimetic remineralization of the surface of demineralized dental enamel using HAP@ACP nanoparticles guided by glycine. Sci Rep 2017; 7: 40701.

Weir M, Chow L, Xu H. Remineralization of demineralized enamel via calcium phosphate nanocomposite. J Dent Res 2012; 91(10): 979-984.

Zoellner A, Diemer B, Weber HP, Stassinakis A, Gaengler P. Histologic and radiographic assessment of caries-like lesions localized at the crown margin. J Prosthet Dent 2002; 88(1): 54-59.

Table 1 Means, standard deviations, and the values of a 95% confidence interval of Vicker microhardness of enamel (E) in 1A and cementum (C) in 1B before demineralization (B_D), after demineralization (A_D), and after remineralization (A_R) with nanohydroxyapatite (N_{HA}), Clinpro (C_P), or without treatment (N_T)

(1A) Vicker microhardness of enamel (E)

Group	n	Mean	Standard deviation	95% Confidence Interval	
				Lower Bound	Upper Bound
EN_TB_D	10	377.3690	22.99676	360.918	393.820
EN_TA_D	10	161.9490	10.54402	154.406	169.492
EN_TA_R	10	161.6940	5.92586	157.455	165.933
$EN_{HA}B_D$	10	378.2000	18.76017	364.780	391.620
$EN_{HA}A_D$	10	160.7270	8.38881	154.726	166.728
$EN_{HA}A_R$	10	200.0780	8.29663	194.143	206.013
EC_PB_D	10	380.5350	25.14572	362.547	398.523
EC_PA_D	10	161.9420	5.65927	157.894	165.990
EC_PA_R	10	193.1670	7.54709	187.768	198.566

(1B) Vicker microhardness of cementum (C)

Group	n	Mean	Standard deviation	95% Confidence Interval	
				Lower Bound	Upper Bound
CN_TB_D	10	60.3740	3.81789	57.643	63.105
CN_TA_D	10	17.6580	0.91562	17.003	18.313
CN_TA_R	10	17.0440	1.00634	16.324	17.764
$CN_{HA}B_D$	10	62.5880	3.37131	60.176	65.000
$CN_{HA}A_D$	10	18.3890	1.33461	17.434	19.344
$CN_{HA}A_R$	10	27.9930	2.68884	26.070	29.916
CC_PB_D	10	62.8720	4.75316	59.472	66.272
CC_PA_D	10	19.0750	1.30860	18.139	20.011
CC_PA_R	10	24.4680	2.02409	23.020	25.916

Table 2 Analysis of variance (ANOVA) and contrasts of microhardness upon different materials and stages of application for enamel (E) in 2A and cementum (C) in 2B before demineralization (B_D), after demineralization (A_D), and after remineralization (A_R)

(2A) ANOVA of Vicker microhardness of enamel (E)

Source	Sum of squares	Designed factor	Mean square	F-score	*p*-value
Intercept	1753148.440	1	1753148.440	16271.160	0
Material	983.015	2	491.507	4.562	0.020
Error	2909.135	27	107.746		

Contrasts of microhardness of enamel (E) before demineralization (B_D), after demineralization (A_D), and after remineralization (A_R)

Source	Measurement	Sum of Square	Designed Factor	Mean Square	F-score	*p*-value
Stages	B_D vs. A_D	1414780.027	1	1414780.027	3076.973	0
	A_D vs. A_R	16483.477	1	16483.477	404.492	0
Stages * Materials	B_D vs. A_D	51.790	2	25.895	0.056	0.945
	A_D vs. A_R	8752.192	2	4376.096	107.386	0
Error	B_D vs. A_D	12414.495	27	459.796		
	A_D vs. A_R	1100.280	27	40.751		

(2B) ANOVA of Vicker microhardness of cementum (C)

Source	Sum of squares	Designed factor	Mean square	F-score	*p*-value
Intercept	35698.531	1	35698.531	10623.760	0
Material	121.535	2	60.767	18.084	0
Error	90.727	27	3.360		

Contrasts of microhardness of cementum (C) before demineralization (B_D), after demineralization (A_D), and after remineralization (A_R)

Source	Measurement	Sum of Square	Designed Factor	Mean Square	F-score	*p*-value
Stages	B_D vs. A_D	56952.090	1	56952.090	4038.439	0
	A_D vs. A_R	689.569	1	689.569	186.233	0
Stages * Materials	B_D vs. A_D	11.765	2	5.882	0.417	0.663
	A_D vs. A_R	527.414	2	263.707	71.220	
Error	B_D vs. A_D	380.768	27	14.103		
	A_D vs. A_R	99.973	27	3.703		

Table 3 Multiple comparisons of microhardness before demineralization (B_D), after demineralization (A_D), and after remineralization (A_R) of enamel (E) and cementum (C) upon an application of nanohydroxyapatite (NHA), Clinpro (CP), or no treatment (NT)

Stage	Enamel				Cementum			
A_D-B_T		NT	NHA	CP		NT	NHA	CP
	NT	1.000	1.000	1.000	NT	1.000	1.000	1.000
	NHA		1.000	1.000	NHA		1.000	1.000
	CP			1.000	CP			1.000
A_M-A_D		NT	NHA	CP		NT	NHA	CP
	NT	1.000	0	0	NT	1.000	0	0
	NHA		1.000	.025	NHA		1.000	0
	CP			1.000	CP			1.000

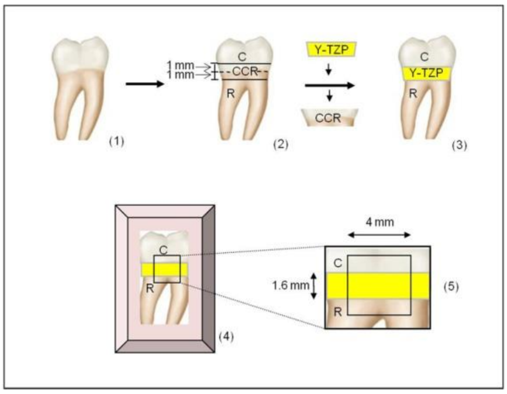

Figure 1 An illustration showing a human third molar (1) sectioned at 1-mm below and above its cemento-enamel junction (2), replaced with an ytria-stabilized zirconia polycrystalline disk (Y-TZP) to the crown (C)-cemento-enamel junction-root (R) portion (CCR) by bonding to the crown and root portions (3), followed by an investment in an acrylic block (4) and a preparation of a smooth 4x4 mm^2area (5)

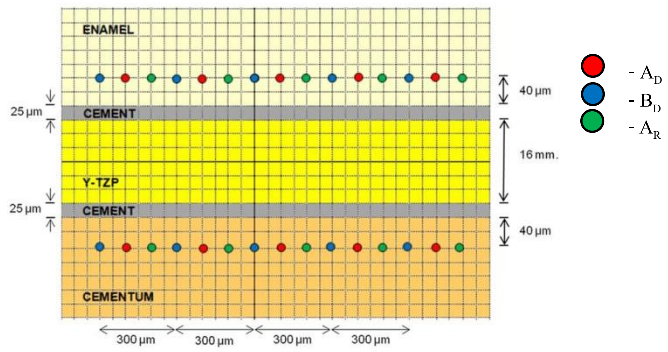

Figure 2 An illustration showing Vicker microhardness obtained at a 40-micron level on the enamel above enamel-resin cement junction and on the cementum below cementum-resin cement junction (five locations each and with a 100-micron distance apart) before demineralization (B_D), after demineralization (A_D), and after remineralization (A_R)

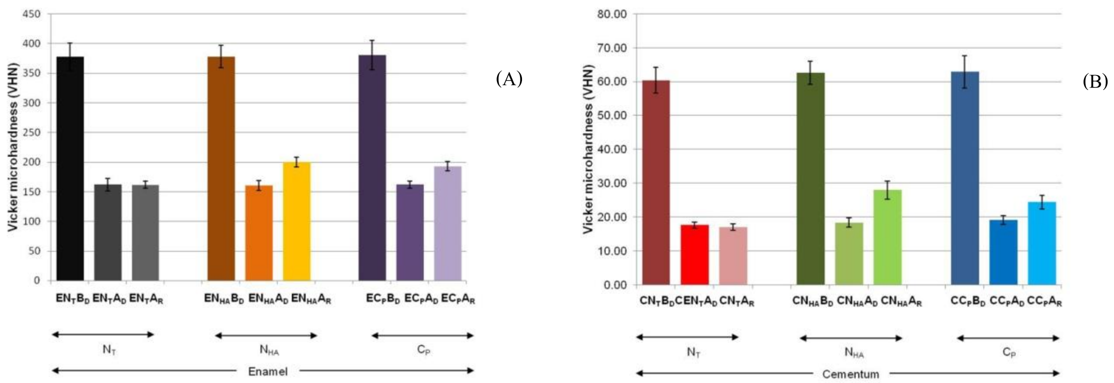

Figure 3 Means and standard deviations of Vicker microhardness of enamel (E) and cementum (C) shown in A and B, respectively, before demineralization (B_D), after demineralization (A_D), and after remineralization (A_R) with nanohydroxyapatite (N_{HA}) or Clinpro (C_P), in comparison with those without treatment

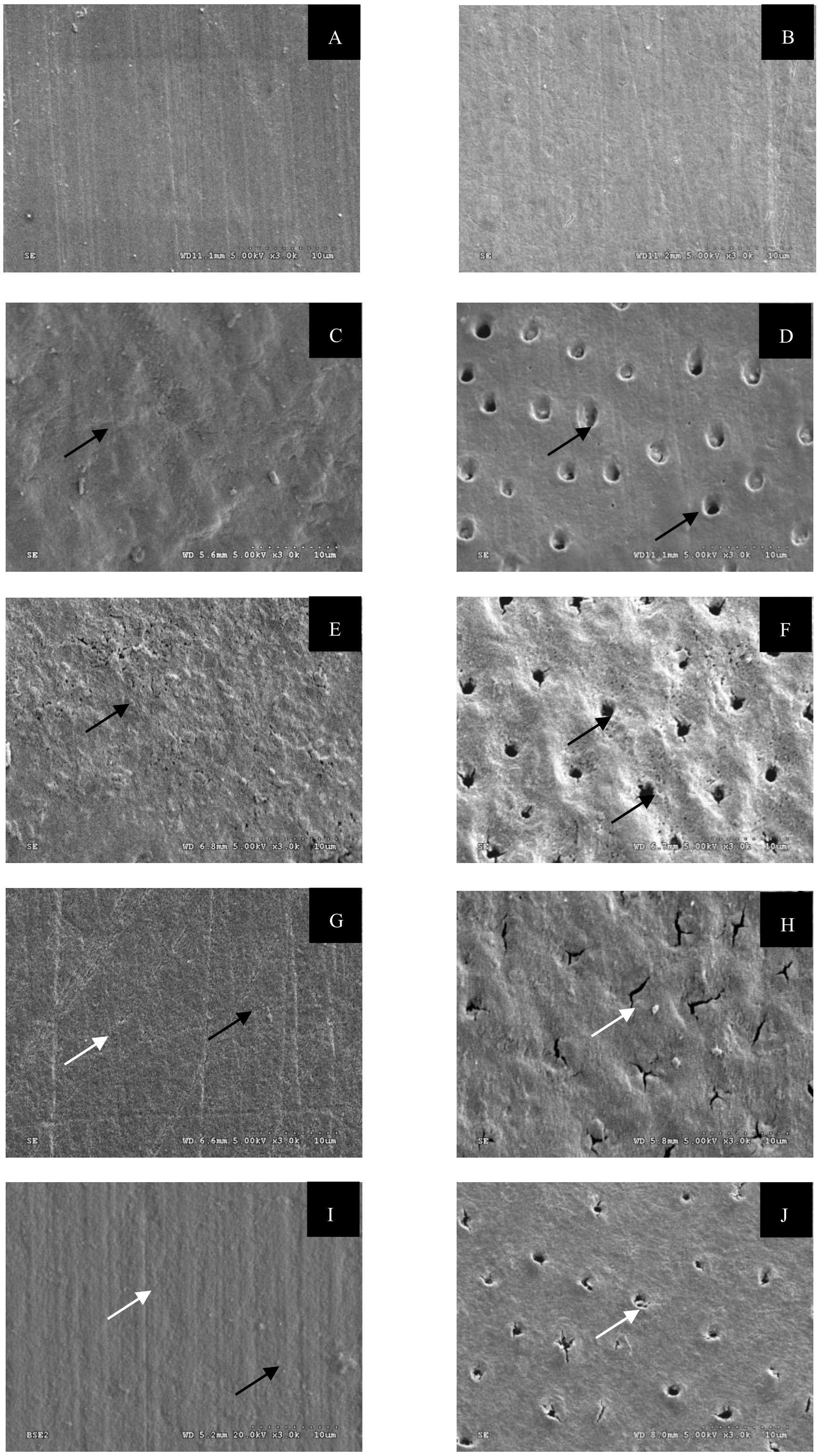

Figure 4 Scanning electron micrographs showing the surfaces of enamel (left-sided column) and cementum (and right-sided column) before demineralization (A and B), after demineralization (C and D), and after application with NHA (G and H), or CP (I and J), in comparison with those without treatment (E and F). When compared to those with the demineralized surfaces (Black arrows in C-G and I), some more obliterations of the porous surfaces are visible in both enamel and cementum surfaces applied with NHA and CP (White arrows in G-J).